Hyperfine Interactions 1 (1975) 93–112

COVALENCY EFFECTS ON IMPLANTED ^{119}Sn IN GROUP IV SEMICONDUCTORS STUDIED BY MÖSSBAUER AND CHANNELING EXPERIMENTS

G. WEYER *, A. NYLANDSTED-LARSEN, B.I. DEUTCH, J.U. ANDERSEN and E. ANTONCIK
Institute of Physics, University of Aarhus, DK-8000 Aarhus C, Denmark

Received 19 February 1975
(Revised 24 March 1975)

Radioactive ^{119m}Sn has been implanted with an isotope separator in single crystals of germanium, silicon, and diamond. Implantations of low doses ($\sim 10^{13}$ atoms/cm^2) at room temperature were performed as well as of higher doses at temperatures of about 400°C. The Mössbauer spectra of these sources show mainly one line. This line originates from ^{119m}Sn on substitutional lattice sites as determined from channeling experiments with 2 MeV He^+ ions on the same samples. The observed systematics of the isomer shifts for ^{119}Sn is explained on the basis of the average electronic configuration $ns^2 np^2$ characterizing chemical bonding in the host crystals. The Debye-Waller factors measured at room temperature are compared to values calculated in a high temperature approximation which accounts for impurity-host mass difference.

1. Introduction

Ion implantation of impurity atoms in solids by means of isotope separator or nuclear recoil techniques is now one of the standard methods used in hyperfine structure investigations. Some advantages of these methods are: a wide range of isotopically pure impurity and host materials can be chosen unrestricted by problems from diffusion, solubility, competing contaminating radiation etc., well-controlled amounts of material can be implanted at a depth determined by the implantation energy, and a reproducible host-impurity experimental environment accessible to theoretical analysis can be created for much of the implant.

On the other hand, there are two main drawbacks to these methods: the atoms often embed into more than one lattice site and the implantation process frequently is accompanied by radiation damage of the host material. These problems have been obstacles even to some technical applications such as the isotope separator doping of semiconductors. Hence, it has been found useful to combine hyperfine and

* Institut für Atom- und Festkörperphysik, Freie Universität Berlin, D-1000 Berlin 33.

channeling experiments for a more complete understanding of both the implantation process and hyperfine interactions. With the channeling technique [1], the radiation damage can be assessed and the lattice position of the implant may be deduced to supplement the information yielded from the hyperfine interaction experiment.

Combined hyperfine-channeling studies have been made before (for example, see papers in ref. [2]). However, past investigations have been hampered by an inability to use the same crystal for both the location and hyperfine measurements. For the case of ^{119}Sn, Mössbauer effect requirements of high source strength ($\gtrsim$ 10 μCi) is antagonistic to the low-dose requirements ($\lesssim 10^{14}$ atoms/cm^2) for damage free channeling investigations in the semiconductors.

In the present study, the utilization of a resonance counter (parallel-plate avalanche counter) for the Mössbauer measurements made feasible low dose implantation (100 nCi equivalent to $\sim 10^{14}$ atoms/cm^2) so that each implanted crystal could be used for both channeling and Mössbauer studies. Furthermore, the low dose reduced contamination of the isotope separator from the long half-life of ^{119m}Sn ($T_{\frac{1}{2}}$ = 245 d). Hot implantation (400°C) also reduced radiation damage.

Systematic implantations for Mössbauer effect measurements in the group IV semiconductors have been reported by the Stanford group [3] for ^{57}Fe and by Hafemeister and de Waard [4] for ^{129}I. The ^{57}Fe was implanted by the Coulomb excitation recoil technique while ^{129}Te (which decays to ^{129}I) was implanted with an isotope separator. The latter technique was also used by Barros et al. [5] for ^{57}Co in diamond and Sawicki et al. [6] for ^{57}Fe in silicon. In all the previous studies, two main Mössbauer lines were observed with strikingly similar isomer shift systematics in the group IV elements for both implanted nuclei. The lines were tentatively assigned to a substitutional and interstitial site [3, 4].

In a preliminary report [7], we partially confirmed these results, from combined Mössbauer and channeling studies of implanted ^{119m}Te and ^{119m}Sn in the group IV semiconductors [7–9]. In the present paper, more complete Mössbauer and channeling investigations of ^{119m}Sn implanted in group IV elements are reported. In particular, the isomer shifts for ^{119}Sn are explained on the basis of the average electronic configuration $ns^{Z_s}np^{Z_p}$ characterizing chemical bonding in the host crystals. The Debye-Waller factors measured at room temperature are compared to values calculated in a high temperature approximation which includes the impurity-host mass difference in a simple manner.

2. Experimental

2.1. A sample preparation

The ^{119m}Sn ($T_{1/2}$ = 245 d) was implanted at 60 keV energy, temperatures of about 20° or 400°C with the Aarhus separator I. This corresponds to an average depth of

~ 300 Å for the Sn in all samples. The ^{119m}Sn had a specific activity of ~0.1 Ci/g with a content of 2% stable ^{119}Sn; the resultant specific activity of the implant was ~5 Ci/g. The single crystals of the semiconductor samples cut perpendicular to a major axis were tilted by 7° relative to the beam axis to avoid implantation in a channeled direction. The implanted doses were determined from the ion current during the separation as well as from the He^+ backscatter spectra from the channeling experiments. Due to resonance counting (see subsect. 2.2), the resultant necessary sample doses (~50 nCi) minimized the radioactive contamination of the separator to about 5 μCi/separation. All samples were carefully cleaned and polished before implantation. Silicon * and germanium ** were polished mechanically and treated chemically in mixtures of HNO_3 and HF. Special cleaning sequences which included boiling acids (HF, H_2SO_4, HNO_3) were applied to the diamond sample.

2.2. Mössbauer technique

A conventional electromagnetic drive system † (in combination with a TMC 400 multichannel analyser) was used to vibrate the implanted sources. The emitted γ rays were detected in a small resonance detector of the parallel-plate avalanche counter type [11, 12] consisting of two or more parallel plates as electrodes (see fig. 1) in a gas filled housing. The cathodes were covered with the resonance absorber material (SnO_2 or $CaSnO_3$ enriched in ^{119}Sn). At resonance, the increased emission of reemitted conversion electrons increases the count rate above background. The background is due mainly to photoemission from non-resonant γ or X radiation. Signal to background ratios of about 10 : 1 with 10% counting efficiencies of the incoming recoil-free emitted γ radiation were attained. Thus, compared to transmission experiments, spectra with comparable statistical information were collected in a much shorter time with relatively weak sources. (For example, the ^{119m}Sn activity of the diamond sample was 10 nCi; the measuring time was 3 weeks.)

2.3. Channeling apparatus

The Aarhus University 2-MeV Van de Graaff accelerator was used for the channeling experiments. The 2 MeV He^+ ions were directed on the samples mounted in a goniometer. Energy spectra of backscattered ions were measured with a silicon surface-barrier detector at a scattering angle of 135°. As shown in fig. 2, particles scattered by host and impurity atoms are well-separated in energy. The single-crystal targets were aligned with major crystal axes parallel to the incoming beam. Normally, backscattering spectra in these aligned positions and in "random" posi-

* n-type single crystals (7 Ω · cm) from Topsil A/S.
** n-type single crystals (0.01 Ω · cm) from Topsil A/S.
† Groningen type, kindly built by Professor de Waard (ref. [10]).

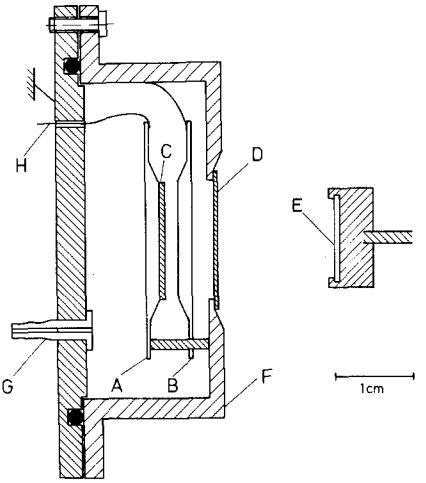

Fig. 1. Schematic view of the resonance detector (parallel-plate avalanche counter type). A,B – parallel plate system (circular lucite plates). A – cathode, B – anode (grounded), C – resonance scattering layer, D – thin entrance window, E – Mössbauer source, F – counter housing (lucite or aluminium), G – gas inlet, H – high voltage feed through.

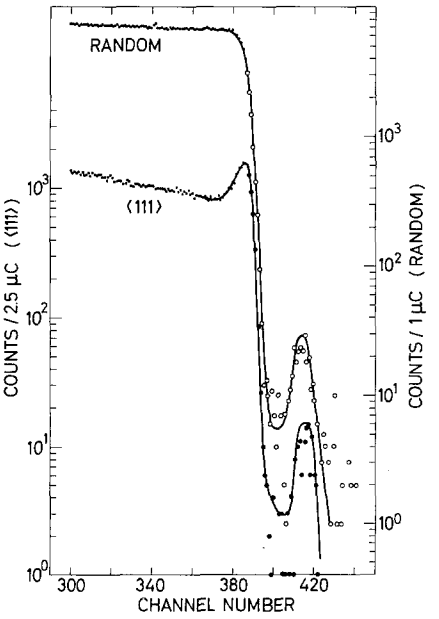

Fig. 2. Energy spectra of 2 MeV helium particles backscattered from an implanted germanium crystal with the incident beam (○) along a random and (●) parallel to the ⟨111⟩ direction.

tions some degrees off the axes were measured. They are compared to yield the channeling effect. In some cases angular scans around the major axes were performed. The relative normalization of the spectra was achieved through beam current integration. A cold trap around the target prevented the deposition of a carbon layer on the targets. A negative voltage was applied to the trap in order to avoid errors in the current integration due to secondary electron emission from the target.

3. Results and data treatment

Fig. 2 displays backscatter spectra measured for random and aligned incidence of the 2 MeV He^+ beam with respect to the indicated axial direction of a germanium host lattice. The separation between the particles scattered from the host atoms (continuous part of the spectra) and those scattered from the heavier ^{119}Sn impurity atoms (peak in the spectrum) allows an unambiguous determination of the minimum yield for the impurity atoms, χ_{imp}. (The minimum yield is defined as the ratio of yields for aligned and random incidence.) The minimum yield for the host, χ_{host}, should be determined at the depth of the impurity, which for the case shown in fig. 2, corresponds approximately to the position of the small peak in the aligned spectrum. Since this sample was heated during implantation, most of the primary damage has been annealed and the peak in scattering yield is probably caused mainly by strain due to the presence of the impurity atoms.

From the minimum yields for the impurity and host, the equivalent fraction E may be calculated,

$$E = (1 - \chi_{imp})/(1 - \chi_{host}) . \quad (1)$$

When the damage is negligible, this fraction is identical to the substitutional fraction. In a previous investigation [13] of the dependence of channeling and Mössbauer experimental results on implantation dose and temperature for ^{119}Sn in silicon, it was suggested that the equivalent fraction is the relevant parameter to compare with microscopic hyperfine measurements, which do not depend sensitively on long range order or disorder. Representative results of this investigation are shown in tables 1 and 2. For hot implants the equivalent fraction is close to unity even for high doses causing considerable lattice strain. Also, for hot implants the Mössbauer parameters are independent of dose and have the same value as for a low-dose cold implant. For higher doses implanted at room temperature (cold), the lattice structure is completely destroyed and a significant line broadening and reduction of the recoil free fraction were observed in the Mössbauer measurements. It was concluded that the isomer shift and recoil free fraction measured for low dose hot implants are those for tin on a regular lattice site in the silicon host lattice with nearly undisturbed surroundings.

For similar implantation conditions, a high equivalent fraction and minor damage are also observed for germanium, as shown in table 1, and the same conclusion may

Table 1
Channeling results of ^{119}Sn in group-IV semiconductors.

Sample	Host	Implanted dose (atoms/cm^2)		Minimum yield *		Equivalent fraction	Implantation temperature (°C)
		from ion curr	from backscattered He^+	host	impurity		
C1	diamond	$5 \cdot 10^{13}$	$\lesssim 1 \cdot 10^{13}$	~0.20			20
C2	diamond	$5 \cdot 10^{13}$	$5 \cdot 10^{13}$	~0.30***	0.60***	0.57 ± 0.1	20
Si1	silicon	$1 \cdot 10^{14}$	$2.2 \cdot 10^{14}$	0.04	0.11	0.93 ± 0.02	400
Si2	silicon	$2 \cdot 10^{15}$	$2.4 \cdot 10^{15}$	0.50	0.50	1.00 ± 0.05	400**
Si3	silicon	$2.4 \cdot 10^{13}$	$\lesssim 1.2 \cdot 10^{13}$	~0.20			20
Ge1	germanium	$1.0 \cdot 10^{14}$	$1.0 \cdot 10^{14}$	0.085	0.20	0.87 ± 0.03	450

* Average of results for ⟨110⟩ and ⟨111⟩ directions.
** See also ref. [13].
*** ⟨110⟩ direction.

Table 2
Mössbauer results of ^{119}Sn in group-IV semiconductors. The isomer shift δ and f factor are defined in the text.

Sample	Host	Substitutional site		f-factor	second site
		δ* (mm/s)	line width (mm/s)		δ* (mm/s)
C1	diamond	1.62(4)	~2.7	0.62(10)	5.0(2)
Si1	silicon	1.84(3)	0.93(4)	0.28(5)	–
Si2	silicon	1.84(3)	0.93(3)	0.28(3)	–
Si3	silicon	1.86(6)	0.94(8)	0.29(4)	–
Ge1	germanium	1.90(4)	0.94(6)	0.22(4)	–
α-Sn		2.01(4)	1.24(6)	–	–

* relative to a SnO_2-source.

be drawn. In the case of diamond, however, the damage cannot be annealed out during implantation. In sample C1, the dose was too low to allow a measurement of the equivalent fraction by the channeling technique, but after a later implant of stable ^{119}Sn (sample C2) it was possible. The result implies that most of the tin atoms are embedded substitutionally in the diamond lattice, and therefore the isomer shift of the main line in the Mössbauer spectrum must correspond to a substitutional site. A significant population of another site cannot be excluded, however. One large uncertainty in the measurement is connected with the evaluation of the host minimum yield. As for the case of a cold low dose implantation in silicon, the damage is high close to the surface, but decreases rapidly with depth. The depth corresponding to the value of χ_{host} given in table 1 was evaluated from the shift of the tin backscatter peak from the edge of a backscatter spectrum from a tin foil. Furthermore, for low dose implants, the average damage at a given depth may not be representative of the immediate surroundings of the impurity atoms.

Mössbauer spectra for ^{119m}Sn implanted in diamond, silicon, and germanium are displayed in fig. 3. A resonance counter with a SnO_2 scatterer was used in these experiments. The spectra for the silicon and germanium hosts are fitted using a least square procedure with two Lorentzian distributions since SnO_2 is known to exhibit a quadrupole splitting of about 0.5 mm/sec. These spectra are compared with a transmission spectrum (inverted) of a thin α-tin* absorber measured at room temperature with a $BaSnO_3$ source. While the line-widths for the single lines of ^{119}Sn in silicon, germanium and α-tin are relatively similar, the diamond line is considerably broadened and there is some evidence for a second component, as indicated in the spectrum.

* We are grateful to Dr. W. Vogl for the α-tin powder.

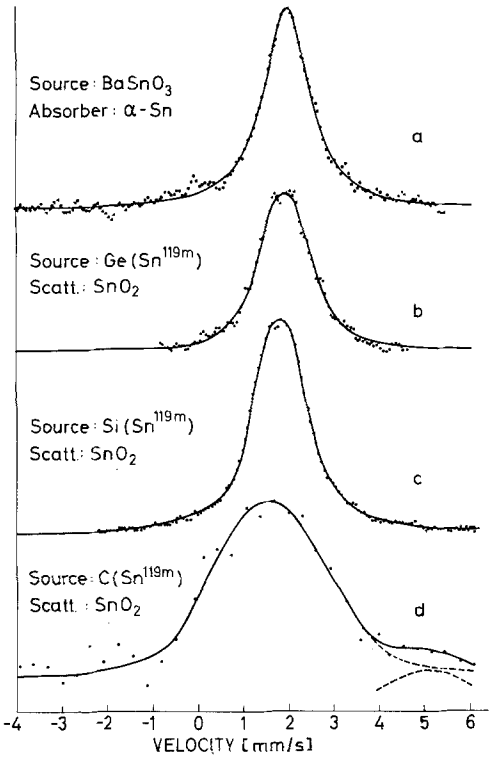

Fig. 3. Mössbauer spectra of ^{119m}Sn implanted in diamond (room temperature, 5×10^{13} atoms/cm^2), silicon (400°K, 10^{14} atoms/cm^2), and germanium (450°K, 10^{14} atoms/cm^2). A transmission spectrum (inverted) of α-tin is included. The velocity scale is given relative to the IS of a SnO_2 source (larger IS corresponds to larger s-electron density).

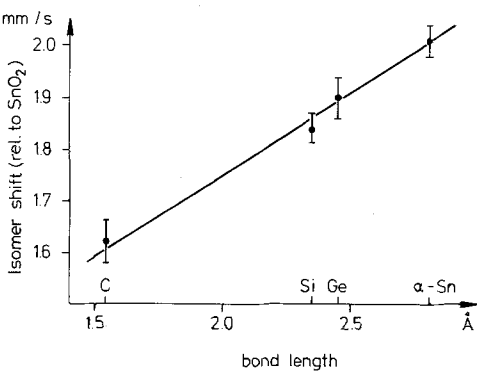

Fig. 4. The isomer shift of implanted ^{119}Sn in group-IV semiconductors vs the bond length of the respective crystal.

The isomer shifts and line widths obtained from the Mössbauer experiments are listed in table 2. The isomer shifts are plotted as a function of the bond length of the host crystal in fig. 4. Because the radioactivity per unit area was weak, the sources were implanted over a relatively large area, about 0.8 cm^2; large solid angles had to be used to shorten the measuring time. The geometric corrections of the measured isomer shift and line width were evaluated experimentally. All sources were measured in the same geometry with the same resonance counter. To avoid errors from drifts in the apparatus, a reference source of ^{119m}Sn in Si was repeatedly remeasured. For this sample, the influence of the source to counter distance was studied experimentally and the velocity scale was calibrated using the magnetic splitting of ^{57}Fe in iron as a reference.

The spectra of implanted silicon and germanium samples could be satisfactorily fitted with two Lorentzians although the observed line widths are somewhat broader (~40%) than the natural line width $2\Gamma_0$. The spectra from diamond samples are considerably broadened ($\sim 5\Gamma_0$) so that the quadrupole splitting of the SnO_2 resonance counter is small compared to this width. To determine the area of these lines and the isomer shift, these spectra were fitted with two or three relatively broad Lorentzians.

The relative recoilless fractions for these implanted sources can be determined from the areas of the resonance curves. Corrections for finite absorber thickness are negligible since the thickness is determined by the shallow range of the conversion electrons. The effective thickness for a single line absorber is given by

$$T_a = \rho_N d f_a \sigma \,, \tag{2}$$

where ρ_N is the density of resonant atoms, d is the thickness of the resonance layer, f_a is the Debye-Waller factor of the absorber, and σ is the maximum resonance cross section. The effective thickness for the SnO_2 layer (taking the quadrupole splitting into account) is low ($T_a \lesssim 0.4$). Also, self-absorption in the source can be neglected since the effective thickness is only $T_s \approx 10^{-4}$ for an implanted dose of 10^{14} atoms/cm^2. For a "thin" source and absorber, the area F of the resonance curve (normalized to a source decay rate $N_0 = 1$) is given by

$$F = \tfrac{1}{2}\pi\, T_a \Gamma_{exp} \epsilon f_s \,. \tag{3}$$

Here, f_s is the Debye-Waller factor of the source, Γ_{exp} is the experimentally observed line width, and ϵ is the overall efficiency of the resonance detector for recoilfree γ-radiation. If the effective thickness, efficiency, and the Debye-Waller factor of the absorbing material in the resonance counter, and the strength of the source were accurately known, the Debye-Waller factor for the source could be determined directly from the measured spectrum. However, in general these parameters are too imprecisely determined.

The background in the Mössbauer spectra is due to electrons emitted from nonresonant interactions of X and γ rays; it stems mainly from the photoeffect in the resonance counter from the source or room background radiation. The energies

and relative intensities of the radiation emitted from the sources are almost the same for all the implantations except for differences in the characteristic X rays of the host materials. However, these X rays can be neglected; they are absorbed in the entrance window of the counter. Therefore, the different source strengths can be normalized from the background radiation of their respective measured spectra. From determinations with the same resonance counter, the relative f-factors are then derived from the normalized areas of sources 1 and 2 by use of the ratios

$$\frac{f_s^{(1)}}{f_s^{(2)}} = \frac{F^{(1)}}{F^{(2)}} \,. \tag{4}$$

Here

$$F = \int_{-\infty}^{\infty} \frac{I(v) - I(\infty)}{I(\infty)} \, \mathrm{d}v \,,$$

where $I(v)$ is the counting rate at source velocity v, and $I(\infty)$ is the counting rate at high source velocity, where resonance is absent. (The contribution from the room background radiation must be subtracted.)

If the energy spectrum of the recoilless radiation emitted from the source is not a Lorentzian, eq. (4) still is correct [14]. Also, a quadrupole splitting in the absorber material does not affect this relationship. However, if the spectral distributions of the sources and absorber are not well approximated by Lorentzian shapes (as is the case for ^{119}Sn in diamond), it is difficult to determine the area F to better than 5–10% accuracy.

To convert the relative Debye-Waller factors into absolute values, a spectrum from a source with a known Debye-Waller factor must be measured. The source must have a pure ^{119m}Sn γ- and X-ray spectrum with negligible self-absorption. Recently, Müller et al. [15] determined the Debye-Waller factor for the 159 keV transition of ^{117}Sn in a SnO_2 matrix. Using this value they deduced the Debye-Waller factor for the 24 keV transition of ^{119m}Sn in the same matrix for a SnO_2 source carefully prepared from irradiated highly enriched ^{118}Sn [16]. This source yielded $f = 0.28 \pm 0.03$ in agreement with another recent determination of $f = 0.28 \pm 0.03$ [17]. The Müller et al. source was used to calibrate the resonance detector. The spectrum of the 24 keV γ and X rays emitted from the calibration source and the implanted silicon source were compared with a high resolution germanium detector. Any self-absorption would have changed the γ to X-ray ratio but they were the same for both sources to within 1%. The Debye-Waller factors obtained from the areas of the measured spectra are also listed in table 2.

4. Electronic structure of the impurity

The interpretation of these measurements in terms of the electronic structure relies on the well-known formula for the isomer shift (IS):

$$\delta = \frac{2\pi e^2 c}{5} \frac{ZR^2}{E_\gamma} \left(\frac{2\delta R}{R}\right) [\rho^e(0) - \rho^a(0)] \ . \tag{5}$$

Here, Z is the nuclear charge, E_γ the energy of the resonant gamma quantum, $\delta R/R$ the relative change of the effective nuclear radius $R = 1.2\, A^{\frac{1}{3}}$. The quantities $\rho^e(0)$ and $\rho^a(0)$ represent the relativistic electron probability densities at the nucleus for emitter and absorber. Since the electron states of the core electrons are usually not affected by chemical bonding, the last factor in the above formula depends mainly upon the densities of the valence electrons. The IS thus reflects the difference between two configurations of the valence electrons due to the change in chemical environment around the emitting and absorbing nuclei.

It is well known that substitutional tin atoms represent isoelectronic impurities which have in the atomic state the same valence electron configuration ns^2np^2 as C, Si, and Ge. Moreover, α-tin crystallizes in the diamond structure with simple covalent bonding as do group IV semiconductors. Thus it can be expected that a single impurity tin atom will cause only a very small deformation of the band structure of the host crystals.

Unfortunately, there is little experimental information concerning Sn impurities in group IV semiconductors. It is assumed here that substitutional Sn impurities produce no bound states in the forbidden gap of these materials. Theoretical calculations for silicon by Baldereschi and Hopfield [18] confirm the absence of bound states. It will be shown presently that the IS measurements are consistent with this assumption. Furthermore, one can assume that the wave functions of the valence electrons of a tin impurity atom substitutionally embedded in a group IV semiconductor hybridize with the relevant orbitals of the neighbouring atoms of the host crystal in order to reproduce the host's electronic configuration as much as possible.

The actual calculation of the IS, that is to say of the change of the electron density at the tin nucleus, is a complex problem. In general, one should know the relativistic solutions of the Sn impurity problem in group IV semiconductors. Unfortunately, this problem is far from solved. Here an attempt will be made to explain, in a semiquantitative way, the general trend of the IS results by using a simple tight binding model of the unperturbed band structure of the host crystal [19].

All group IV semiconductors and also α-Sn crystallize in the diamond structure which is composed of two interpenetrating face-centered cubic lattices displaced along the body diagonal by one fourth of its length, i.e. by a vector $\tau = a(1/4, 1/4, 1/4)$. Then the solutions of the Schrödinger equation can be written in the following form:

$$\psi_{\nu k}(r) = \frac{1}{\sqrt{2N}} \sum_j \sum_{n=s,x,y,z} e^{ik \cdot R_j} [C_{\nu k}(n) a_n(r - R_j) + C'_{\nu k}(n) e^{ik \cdot \tau} a_n(r - R_j - \tau)] \tag{6}$$

Here, $2N$ is the number of atoms in the volume of the crystal and a_s, a_x, a_y, a_z are

the normalized atomic (or Wannier) s and p functions of the valence electrons centered on the lattice sites of the two FCC sublattices denoted by $\boldsymbol{R}_j$ and $\boldsymbol{R}_j + \boldsymbol{\tau}$, respectively. Since these two sublattices are equivalent, $|C_{\nu\boldsymbol{k}}(n)|^2 = |C'_{\nu\boldsymbol{k}}(n)|^2$. For simplicity it is assumed that the a_n's centered on different atoms are "pseudo-orthogonal". The band indices $\nu = 1-4$ describe the occupied valence bands, while the conduction bands are characterized by $\nu = 5-8$.

Since mainly the s-electrons contribute to $\rho^e(0)$ or $\rho^a(0)$, the valence electron probability density at the nuclei in α-Sn or group IV semiconductors can be written as

$$\rho_s(0) = Z_s |a_s(0)|^2 \,. \tag{7}$$

Here, Z_s represents the number of electrons in the state described by the wave function $a_s(r)$. Taking into account the normalization of the $\psi_{\nu\boldsymbol{k}}$'s one can immediately write the following relation

$$Z_s = 2\,\frac{1}{2N} \sum_{\nu=1}^{4} \sum_{\boldsymbol{k}} |C_{\nu\boldsymbol{k}}(s)|^2 \,. \tag{8}$$

It should be noted that in this approximation the average electronic configuration of the valence electrons in group IV crystals is

$$\mathrm{ns}^{Z_s}\mathrm{np}^{Z_p} \,, \tag{9}$$

where

$$Z_s + Z_p = 4 \,. \tag{10}$$

Unlike in the atomic configuration, in crystal material the Z_s and Z_p are no longer integers.

Taking the isomer shift of α-tin as a reference point, that is, supposing that α-Sn is the absorber, $\rho_s^a(0)$ in eq. (5) can be written as

$$\rho_s^{\mathrm{Sn}}(0) = Z_s^{\mathrm{Sn}} |a_s^{\mathrm{Sn}}(0)|^2 \,, \tag{11}$$

where Z_s^{Sn} has to be calculated using eq. (8). If the tin atom is embedded as a substitutional impurity in the crystal lattice, then in the framework of the tight binding approximation the contact density $\rho_s^e(0)$ can be written as follows:

$$\rho_s^{\mathrm{IV:Sn}}(0) = Z_s^{\mathrm{IV:Sn}} |a_s^{\mathrm{Sn}}(0)|^2 \,. \tag{12}$$

Here the superscript IV : Sn means a single Sn-impurity in a group IV semiconductor lattice. It has been already mentioned that in general the calculation of $Z_s^{\mathrm{IV:Sn}}$ requires the knowledge of the solutions of the impurity problem which is rather complicated. It will be discussed in a later paper [20]. For the present purpose, however, a simple estimate of $Z_s^{\mathrm{IV:Sn}}$ can be given based on the following argument: If the host atoms would have the same influence on the tin atom as in α-Sn then

$$Z_s^{IV:Sn} = Z_s^{Sn} . \tag{13}$$

On the other hand if the impurity tin atom would be treated in the same way as the replaced atom of the host crystal then

$$Z_s^{IV:Sn} = Z_s^{IV} . \tag{14}$$

Let us assume that the real case lies somewhere between Z_s^{IV} and Z_s^{Sn}. Using a linear interpolation, one can write

$$Z_s^{IV:Sn} = Z_s^{IV} + k(Z_s^{Sn} - Z_s^{IV}) , \tag{15}$$

where k represents a measure of the degree to which the bonds of the host crystal influence the redistribution of the electron charge at the tin atom subject to condition (10). Consequently, the contact density term in eq. (5) can be written as follows:

$$[\rho_s^{IV:Sn}(0) - \rho_s^{Sn}(0)] = (1-k)(Z_s^{IV} - Z_s^{Sn})|a_s^{Sn}(0)|^2 . \tag{16}$$

This formula implies that, in the tight binding approximation used, the IS is due to the difference between the electronic configuration around the impurity Sn atom and Sn atoms in crystalline α-Sn and is proportional to $(Z_s^{IV} - Z_s^{Sn})$.

The calculation of Z_s^{IV} according to eq. (8) is straightforward but tedious. It cannot be reproduced here and only the resulting values of $(Z_s^{IV} - Z_s^{Sn})$ are given in table 3 (see ref. [19] for more details). Note that the negative values of $(Z_s^{IV} - Z_s^{Sn})$ are in agreement with the present theory of the chemical bond in group IV semiconductors [21, 22]. The decreasing values of Z_s^{IV} when going from α-Sn to Ge, Si, and diamond, respectively, correspond, according to eq. (10), to increasing values of Z_p; this means, however, that the number of p-like electrons with their charges concentrated in covalent bonds decrease when going from diamond to Si, Ge, and α-Sn which corresponds to a weakening of the covalent bonds.

Assuming that k in eq. (15) has approximately the same value for all group-IV semiconductors, it is possible to express the IS in the following way:

$$\delta = C(Z_s^{IV} - Z_s^{Sn}) , \tag{17}$$

where the constant C includes all remaining expressions from the right-hand side of eqs. (5) and (16). Using the most reliable IS measurement of Sn in silicon in

Table 3
Comparison of calculated and measured values of the isomer shift δ relative to ^{119}Sn in α-tin.

Host	$Z_s^{IV} - Z_s^{Sn}$	δ_{th} (mm/s)	δ_{exp} (mm/s)
diamond	−0.278	−0.36	−0.39(6)
Si	−0.133	−0.17	−0.17(4)
Ge	−0.102	−0.13	−0.11(6)
α-Sn	0	0	0

order to estimate C, the corresponding IS values for diamond and Ge can be calculated. They are listed in table 3 and show a reasonable agreement with the relevant experimental values.

In summary it can be said that the magnitude of the IS of the substitutionally implanted tin in group IV semiconductors (measured with respect to α-tin) reflects the strength of the covalent bonding in these materials.

5. Impurity dynamics

The vibrations of the resonance atoms affect both the amplitude of the observed resonance peak and its position. The effect on peak height is represented by the probability that resonance gamma-ray emission or absorption will occur without phonon emission or absorption and is given by the well-known Debye-Waller factor

$$f = \exp[-\tfrac{1}{3}\kappa^2\langle u^2\rangle] \ . \tag{18}$$

Here κ is the wave vector of the gamma ray and $\langle u^2\rangle$ is the mean square displacement of the resonance atom from its equilibrium position. The displacement of the peak position is called the second-order Doppler shift (SOD) and is given by

$$\delta_{\mathrm{SOD}} = \frac{-\langle \dot{u}^2\rangle}{2c} \ , \tag{19}$$

where $\langle \dot{u}^2\rangle$ is the mean square velocity of the emitting atom.

In the following, the vibrations of a crystal are considered in the harmonic approximation, and only zero-phonon processes. The specific emphasis in this section will be directed, naturally, towards the understanding of the dynamics of an isoelectronic impurity like ^{119}Sn in group IV semiconductors vibrating at room temperature. For this case, $M' > M$, where M' and M are the mass of the impurity and host (see eq. (20)), respectively.

Since the Debye-Waller factor depends on $\langle u^2\rangle$ and the SOD depends on $\langle \dot{u}^2\rangle$, only the physical features of these two parameters of the impurity need to be discussed. In general, the quantities $\langle u^2\rangle$ and $\langle \dot{u}^2\rangle$ depend on: (a) the impurity-host mass difference, (b) a difference in force constants between the impurity and the host, and (c) the distortion (relaxation) of the lattice due to the larger impurity core.

With respect to (a) it turns out that the influence of the impurity-host mass difference has to be taken into account properly. Dawber and Elliot [23] have found that there exist no localized states for $M' > M$ and that the resonance modes which might considerably affect the phonon spectrum of the host crystal at some frequencies, have little effect on the mean thermal impurity displacement and velocity. With respect to (b), there is no direct proof that for isoelectronic substitutional Sn impurities in group IV crystals the force constants are changed. There exists, however, some information concerning isoelectronic impurities in $A^{III}B^{V}$ semiconduct-

ing compounds having $M' < M$ and core size smaller than the core of the host atoms. Grimm [24] has shown that in these materials, which have a band structure very similar to that of group-IV semiconductors, the force constants change only by a few percent *and* are independent of the size of the impurity. Although in our case the impurity core size is larger, we have assumed for simplicity that the situation is similar for group-IV host crystals so that only the impurity-host mass difference has been taken into account. However, it will appear that this model is not complete enough to explain the experimental findings.

5.1. Debye-Waller factor

Changes of the Mössbauer parameters f and δ_{SOD} due to mass differences have been treated by a number of authors [23, 25–29]. The high temperature approximation of the Debye-Waller factor as described by Maradudin and Flinn [26], eqs. (4.11)–(4.13) of this paper, reads as follows,

$$f = \exp\left\{-\left(\frac{kT}{M}\,\kappa^2\mu_{-2}\right)\left[1 + \frac{1}{12}\,\frac{M}{M'}\,\frac{1}{\mu_{-2}}\,\frac{\hbar^2}{(kT)^2} + O(\hbar^4)\right]\right\}. \tag{20}$$

Only the first term in (20) is needed as long as the temperature T satisfies the following inequality

$$T \gg \frac{\hbar}{k}\sqrt{\frac{1}{12}\,\frac{M}{M'}\,\frac{1}{\mu_{-2}}} = T_c\,. \tag{21}$$

In the above formulas, $\kappa^2 = E^2/\hbar^2c^2$, where E is the energy of the gamma ray, k and $\hbar$ are the Boltzmann and Planck constants, respectively. The μ_i's are the moments of the unperturbed phonon distribution functions, defined as follows:

$$\mu_2 = \frac{1}{6N}\sum_{kj}\omega_j^2(\boldsymbol{k})\,, \tag{22} *)$$

$$\mu_{-2} = \frac{1}{6N}\sum_{kj}\omega_j^{-2}(\boldsymbol{k})\,. \tag{23} *)$$

In the high temperature limit (eq. (20), first term in the exponential), f depends only on the mass of the host. It is independent of the mass of the impurity, force constant changes and size of the impurity. The second (correction) term is proportional to the host-impurity mass ratio (also, possible host-impurity force constant changes would affect the second-order term).

Numerical values of μ_2 and μ_{-2} calculated for diamond, silicon, and germanium by Dolling and Cowley [30] as well as f and the critical temperature T_c are listed in

* The μ_2 and μ_{-2} as defined by Maradudin and Flinn [eq. (3.27)] relate to the FCC lattice; it can be shown, however (see Dawber and Elliot [23]) that for the diamond lattice the present definition has to be used.

Table 4
Comparison of calculated and experimental Debye-Waller factors at T = 300 K for Sn in different host crystals. The f_{theor} is calculated from eq. (20).

Host	$\mu_{-2} 10^{29} s^{-2}$	$\mu_2 10^{-27} s^2$	$T_c K^0$	f_{theor}	f_{exp}	f_{theor}/f_{exp}
C	4.85	36.2	100	0.85	0.62(10)	1.4
Si	70.3	4.82	40	0.40	0.28(3)	1.4
Ge	221	1.62	36	0.33	0.22(4)	1.5
α-Sn	(500)	(0.70)		(0.21)	0.16(3)*	(1.3)

* From ref. [31].

table 4. Since the corresponding values for α-Sn are not known, a scaling procedure has been used based on the experimental values of the maximum phonon frequencies and the similarity of the phonon spectra for Si, Ge, and α-Sn. Due to the general character of the phonon density of states, the value of μ_2 seems to be more accurate than that of μ_{-2}.

As can be seen from the values of T_c at room temperature in table 4, the second term in eq. (20) is not negligible for all host crystals. In particular a first-term approximation would be too rough for the diamond host. Theoretical values f_{theor} calculated from eq. (20), which include the second term, are listed in table 4 together with the experimental values f_{exp} (column 6). The experimental values are systematically lower than the theoretical values. Only the statistical experimental errors for f_{exp} have been listed in table 4. In addition, there are possible systematic uncertainties due to implantation into damaged or distorted regions (± 10%) and in the calibration of the absolute value of the f factors (± 10%); both uncertainties would tend to lower the experimental f values but hardly by more than about 10%.

On the other hand, the question arises whether the systematic deviation could be accounted for either by inaccurate values of μ_{-2} due to inadequacies in the lattice model used in the low-frequency region (see discussion in ref. [30]) or by including into eq. (20) the force constant changes that have been hitherto neglected. Fortunately, there is experimental evidence that a similar decrease of the f factor is obtained for two cases in which force constants changes are absent. First, Golovin et al. [31] measured the f factor for the 24 keV transition of ^{119}Sn in α-tin (which follows the systematics) listed in table 4. Second, Zimmermann et al. [32] determined the f factor for the 67 keV transition of ^{73}Ge in germanium; from this, the derived value of $\mu_{-2} = (2.52 \pm 0.16) \times 10^{-27}\ s^2$ leads to an f factor of $f = 0.28$ for the case of the 24 keV transition of ^{119}Sn in germanium, in better agreement with, but nevertheless still higher than our experimental value of f. A similar situation can be expected for silicon and diamond; the remaining discrepancy between theory and experiment is probably due to the neglect of the relaxation of the lattice by the larger Sn ion. However, taking into account all possible experimental errors and theoretical approximations, no definite conclusions can be drawn

Table 5
Calculated second-order Doppler shifts from eq. (24).

Host	δ_{SOD}(mm/s)	Δ_{SOD}(mm/s)
C	−0.125	0.017
Si	−0.110	0.002
Ge	−0.109	0.001
α-Sn	−0.108	(0.000)

for the moment. Clearly, further experimental and theoretical investigations are needed.

5.2. The second-order Doppler shift

The first two terms of the δ_{SOD} calculated by Maradudin et al. [33] [eq. (4.36)] in the high-temperature limit are:

$$\frac{-\langle \dot{u}^2 \rangle}{2c} = \frac{-3kT}{2M'c}\left\{1 + \frac{1}{12}\left(\frac{\hbar}{kT}\right)^2 \frac{M}{M'}\mu_2\right\}. \tag{24}$$

Numerical values of δ_{SOD} computed from eq. (24) are listed in table 5. The μ_2 values necessary to determine the SOD of α-tin have been estimated from the value of μ_2 of germanium using the scaling procedure. Since the error of the SOD from a similar scaling procedure for Ge or Si is only −0.005 mm/s, the estimated SOD for α-tin should have a negligible error. The last column of table 5 lists $\Delta_{SOD} = \delta_{SOD_{\alpha\text{-}Sn}} - \delta_{SOD_{IV}}$ which has a magnitude equal or less than the experimental error of the measured isomer-shift differences. Nevertheless, these small corrections have been applied to the measured isomer shifts listed in table 2.

6. Discussion

The aim of this work is to understand the character of the chemical bonding of Sn impurities in group IV semiconductors. The measurements contained in this work make it possible to study both the vibrational states and the internal electronic structure of the impurity atom as influenced by the host. These properties depend sensitively on the position of the impurity atom in the unit cell. Fortunately, the problem has been simplified since the impurity ^{119}Sn in group IV semiconductors can easily be embedded in a substitutional site by implantation into these lattices. The studies have been undertaken by combined Mössbauer measurements (with resonance counting) and channeling on the same crystals; this has been essential. Channeling has shown that the actual Sn studied is implanted to ~90% into the substitutional sites in silicon and germanium and at least to ~60% in

diamond. The knowledge of the location allows quantitative analysis of the main measured Mössbauer parameters of the Sn atoms: (i) the isomer shift, which correlates the electronic structure of the host crystal and the impurity atom with the *position* in the lattice cell, and (ii) the Debye-Waller factor, which depends upon the character of the interatomic forces influencing the dynamics of the impurity.

The advantage of using substitutional Sn is that it is an isoelectronic impurity having no localized donor or acceptor levels. In sect. 4, it has been shown that the redistribution of the valence electrons of the tin atoms having s and p character due to the influence of the host crystal explains the measured isomer shifts in the group IV semiconductors (see refs. [19, 20] for more detail). With respect to lattice dynamics, it has been shown in sect. 5 that the calculated high-temperature approximation to the Debye-Waller factor taking into account only the impurity-host mass difference is systematically higher than the experimental values. However, additional experimental and theoretical information is necessary to clarify the problems.

The question arises to what extent these results are general for the behaviour of other impurities in semiconductors or similar materials. Unfortunately, there exists little reliable *systematic* data for other cases. However, Hafemeister and de Waard [4] have shown that substitutional I which probably forms a complicated multilevel deep donor impurity, has a similar IS variation in diamond, Si, and Ge as Sn. This implies that an analogous redistribution of valence electrons of the iodine atoms takes place (again, see ref. [20] for more detail). One would expect similar results for different donor impurities in group IV semiconductors and α-Sn. Unfortunately, the Debye-Waller factors have not yet been measured for I. This supplemental information is important for ascertaining the effect on the phonon spectra from impurity-host mass differences, impurity size, etc. However, the picture may change for acceptor impurities due to the difference in its electronic configuration.

From what has been stated regarding the substitutional impurities, large changes can be expected with interstitial impurities. For this case, the knowledge of the exact location of the atom in the crystal lattice, so far, has been experimentally elusive. Although preliminary systematic studies utilizing similar techniques are or have been investigated for ^{120}Te [4], ^{119m}Te [7], ^{57}Co [8], and ^{57}Fe [3], each of which has at least one interstitial component in group IV semiconductors, the position and fractional amount at the interstitial site is not known completely.

Besides the previous questions, some additional points emerge from this study that are worth mentioning. The expected increase of isomer shift due to the contraction of the diamond lattice structure from α-tin to diamond is of minor importance for the substitutional site compared with electronic redistribution effects. On the other hand, for interstitial lattice positions, these contraction effects are of major importance.

No difference has been observed in the Mössbauer spectra for ^{119}Sn between low-dose room-temperature and high-temperature implantations. This is not in agreement with the recent measurement of Schultz [34] in which donor and

acceptor levels have been found for implanted Sn at room temperature in silicon. However, these local states are not identified in detail.

The large line broadening in the Mössbauer spectrum for ^{119}Sn in diamond may result from several physical features, foremost from some irregularity in the surrounding of the impurity atoms due to the mismatch in size between impurity and host. That Sn does not end up entirely substitutional could also be due to the large difference in covalent radii for Sn and C. The isomer shift measured for Sn in the second site corresponds to that observed from implantations of ^{119m}Te in diamond [7]. The larger line broadening relative to that observed for the β decay $^{129}\text{Te} \rightarrow {}^{129}\text{I}$ may also arise from after-effects, that is, from changes in the atomic shell after internal conversion decay of ^{119m}Sn and the electron capture decay of $^{119m}\text{Te} \rightarrow {}^{119}\text{Sb} \rightarrow$ $\rightarrow {}^{119}$Sn.

It seems unlikely that the broadening of the substitutional line (or the occurrence of the second line) is due to radiation damage since no drastic broadening was observed for high-dose implantations ($>10^{14}$atoms/cm^2) of ^{129}Te [4] in diamond and since the same width was observed for low-dose implantations ($<5 \cdot 10^{13}$atoms/cm^2) of ^{119m}Te. Also, no particular deviation was found for diamond from the observed systematics of the isomer shift and the recoilless fraction. Drastic changes of the latter parameter have been observed in radiation damaged silicon [13].

We wish to thank Professor J.P.F. Sellshop for the diamond and for advice in its cleaning procedure. Professor E. Gerdau and Dr. W. Müller are thanked for the possibility to calibrate the resonance counter with their ^{119m}Sn source and for communicating their experimental results prior to publication. Helpful discussions are appreciated from H.L. Nielsen.

One of the authors, Gerd Weyer, would like to thank his colleagues at the Institute of Physics, University of Aarhus, for the kind hospitality and cooperation extended to him during his stay there. He also appreciates financial support from the Danish Research Council.

References

[1] J.W. Mayer, L. Eriksson and J.A. Davies, Ion implantation in semiconductors (Academic Press, New York and London, 1970).
[2] Hyperfine interactions in excited nuclei, eds. G. Goldring and R. Kalish (Gordon and Breach, New York, 1971).
[3] G.L. Latshaw, Ph.D. Thesis, Stanford University, 1971 (unpublished).
[4] D.W. Hafemeister and H. de Waard, Phys. Rev. B7 (1973) 3014 and in Mössbauer effect methodology, eds. I.J. Gruverman and C.W. Seidel 8 (1973) 151.
[5] F. de S.Barros, D. Hafemeister and P.J. Viccaro, J. Chem. Phys. 52 (1970) 2865.
[6] J.A. Sawicki, B.D. Sawicka, S. Lazarski and E. Maydell-Ondrusz, Phys. Stat. Sol. 57 (1973) K 143.

[7] G. Weyer, B.I. Deutch, A. Nylandsted-Larsen, J.U. Andersen and H. Loft-Nielsen, Proc. Int. Conf. on the applications of the Mössbauer effect, Bendor 1974, J. Phys. (Paris) 12 (1974) C6-297.
[8] G. Weyer, B.I. Deutch, A. Nylandsted-Larsen and J.U. Andersen, Meeting on radiation damage and hyperfine interactions, Dieppe 1974, summary report by H. Bernas in Proc. Int. Conf. on hyperfine interactions studied in nuclear reactions and decay, Uppsala 1974, to be published.
[9] G. Weyer, B.I. Deutch, A. Nylandsted-Larsen and J.U. Andersen, Proc. Int. Conf. on hyperfine interactions studied in nuclear reactions and decay, Uppsala 1974, to be published.
[10] Description of Mössbauer drive unit, type 516S and of mechanical motion system, Manual, Natuurkundig Laboratorium, R.U., Groningen (1971).
[11] J. Christiansen, P. Hindenach, U. Morfeld, E. Recknagel, D. Riegel and G. Weyer, Nucl. Phys. A99 (1967) 345.
[12] G. Weyer, to be published.
[13] G. Weyer, J.U. Andersen, B.I. Deutch, J.A. Golovchenko and A. Nylandsted-Larsen, Rad. Effects 24 (1975) 117.
[14] G. Lang, Nucl. Instr. 24 (1963) 425.
[15] W. Müller, H. Winkler and E. Gerdau, Proc. Int. Conf. on the applications of the Mössbauer effect, Bendor, 1974, J. Phys. (Paris) 12 (1974) C6-375.
[16] W. Müller, E. Gerdau and H. Winkler, private communication.
[17] G. Hembree and D.C. Price, Nucl. Instr. 108 (1973) 99.
[18] A. Baldereschi and J.J. Hopfield, Phys. Rev. Letters 28 (1972) 171.
[19] E. Antoncik, Proc. Int. Conf. on lattice defects in semiconductors, Freiburg 1974, to be published.
[20] E. Antoncik, Phys. Stat. Sol., to be published.
[21] E. Antoncik, Electrons in crystalline solids (IAEA, Vienna, 1973) p. 461.
[22] J.P. Walter and M.L. Cohen, Phys. Rev. B4 (1971) 1877.
[23] P.G. Dawber and R.J. Elliot, Proc. Roy. Soc. A273 (1963) 222.
[24] A. Grimm, Proc. Int. Conf. on lattice defects in semiconductors, Freiburg 1974, to be published.
[25] Yu. Kagan and Ya.A. Iosilevskii, JETP (Sov. Phys.) 15 (1962) 182; 17 (1963) 195.
[26] A.A. Maradudin and P.A. Flinn, Phys. Rev. 126 (1962) 2059;
A.A. Maradudin, in Solid State Phys., eds. F. Seitz and D. Turnbull 18 (1966) 273.
[27] W.M. Visscher, Phys. Rev. 129 (1963) 28.
[28] G.W. Lehmann and R.E. de Wames, Phys. Rev. 131 (1963) 1008.
[29] P.D. Mannheim, Phys. Rev. 165 (1968) 1011.
[30] G. Dolling and R.A. Cowley, Proc. Phys. Soc. 88 (1966) 463.
[31] V.A. Golovnin, S.M. Irkaev and R.N. Kuznin, JETP (Sov. Phys.) 32 (1971) 372.
[32] B.H. Zimmermann, H. Jena, G. Ischenko, H. Kilian and D. Seyboth, Phys. Stat. Sol. 27 (1968) 639.
[33] A.A. Maradudin, P.A. Flinn and S. Ruby, Phys. Rev. 126 (1962) 9.
[34] M. Schulz, Appl. Phys. 4 (1974) 91 and 225.